Supporting Informaiton

Critical strains for lamellae deformation and cavitation during uniaxial stretching of annealed isotactic-polypropylene

Baobao Chang[1,2,*], Konrad Schneider[1], Fei Xiang[1,2], Roland Vogel[1], Stephan Roth[3], Gert Heinrich[1,4]

[1] Leibniz-Institut für Polymerforschung Dresden, D-01069, Dresden, Germany

[2] Institut für Werkstoffwissenschaft, Technische Universität Dresden, D-01069, Dresden, Germany

[3] Photon Science at DESY, Hamburg, Germany

[4] Institut für Textilmaschinen und Textile Hochleistungswerkstofftechnik, Technische Universität Dresden, D-01069 Dresden, Germany

*Corresponding author

Baobao Chang

E-mail: (chang@ipfdd.de; changpse@126.com)

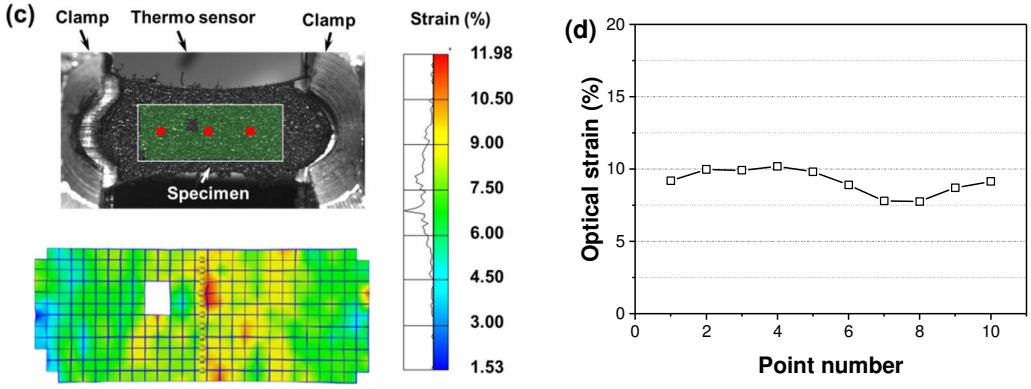

Figure S1 (a) Force-displacement curve and **(b)** stress strain curve of PPna during uniaxial stretching. The stretching temperature is 75 °C. The optical image was taken every 1 second to record the local strain at the beam position (indicated by the yellow cross). The beam position was corrected by a laser before the measurement. **(c)** Photograph of the specimen monitored by the digital image correlation (DIC) system. A sketch of the optical strain in the region of interest is provided. **(d)** The contour of the optical strain in the center region of the specimen.

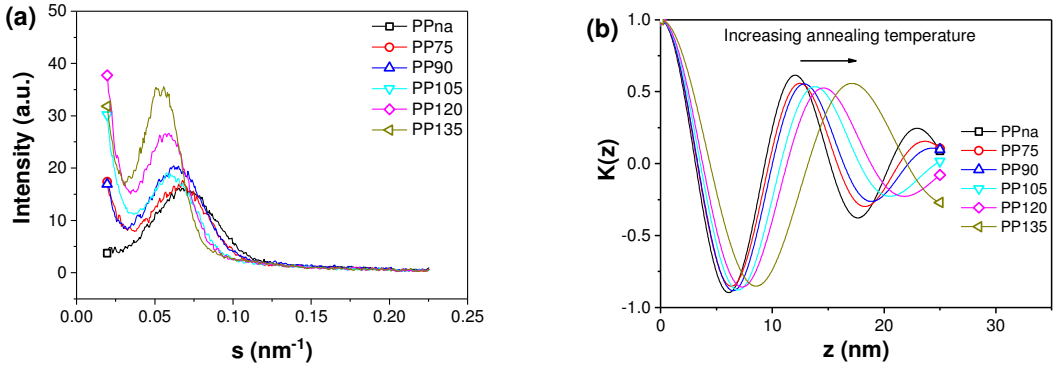

Figure S2 (a) 1D-SAXS curves without Lorentz correction and **(b)** *K(z)* curve of iPP annealed at different temperatures for 6 h.

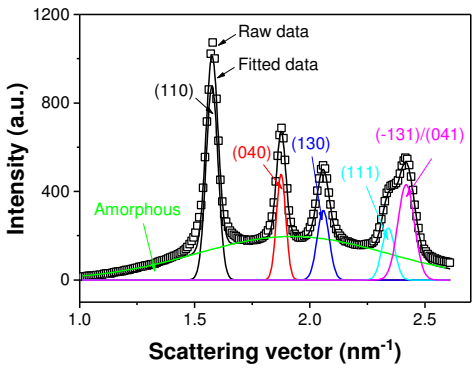

Figure S3 Standard peak fitting procedure for the calculation of crystallinity from the 1D-WAXS curves.

The morphology of PPna after stretching at 75 °C is provided in **Figure S4**. On the image, the lamellae are roughly oriented with their normal along the stretching direction, and a few voids, rather than fibrillary structure, indicated by the yellow arrows can be found. The morphology of the sample verifies that the diamond scattering in the center region of 2D-SAXS pattern of PPna originates from the void.

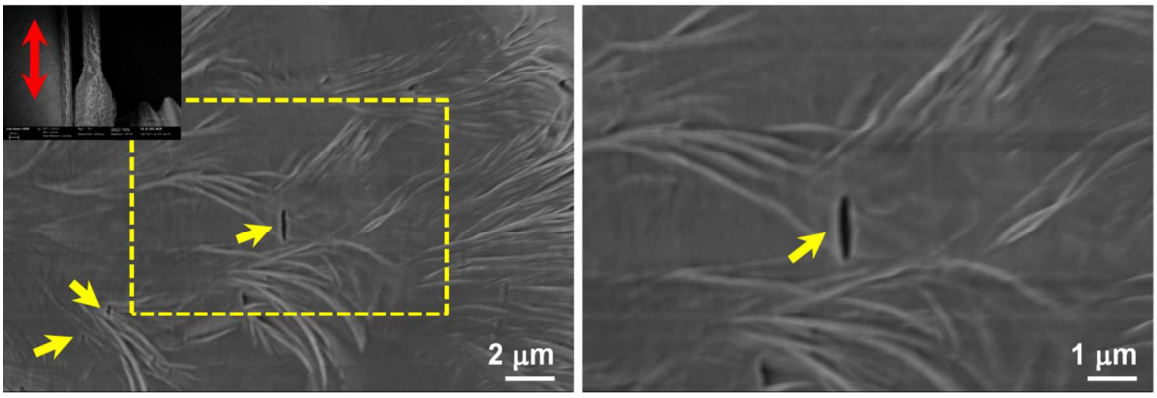

Figure S4 The morphology of PPna after stretching at 75 °C. The yellow arrows are referred to the voids. The Figure inserted in the left image provides geometry of the whole sample (the red arrow indicates the stretching direction). The Figure on the right side is the enlargement of the square region in the left image.

To get the critical strain for lamellae deformation and void evolution during stretching, the in situ SAXS/WAXS measurements and the uniaxial stretching test should be synchronized first. As has been proved by Millot,[1] in the elastic strain range the scattering intensity from the lamellae and crystal over the whole azimuthal distribution always exhibited a heterogeneous feature once the load is applied. The heterogeneous feature at a small strain (0.05) can be also found in **Figure 3** in the manuscript, which is caused by the positive tensile stress in stretching direction and the internal compressive stress perpendicular to stretching because of the Poisson effect. The heterogeneous intensity distribution could be well described by Herman's orientation factor (f_H) as follows[2]

(1) $$\langle cos^2\varphi \rangle = \frac{\int_0^{\pi/2} I(\psi,\varphi) cos^2(\psi,\varphi) \sin(\psi,\varphi) d\theta}{\int_0^{\pi/2} I(\psi,\varphi) \sin(\psi,\varphi) d\theta}$$

(2) $$f_H = \frac{3\langle cos\varphi^2 \rangle - 1}{2}$$

φ is the angle between stretching direction and the normal state of the chosen reference entities (for instance the lamellae and (040) reflection in 2D-SAXS, and 2D-WAXS pattern in this study, respectively), ψ is the azimuthal angle ranging from 0~360 ^{o}. f_H=1 means that the entity is perfectly oriented along the stretching direction, f_H=0 means that the entity is oriented randomly, and f_H=-0.5 means that the entity is oriented perpendicular to the stretching direction. Therefore, f_H could serve as the reference parameter for the start of stretching. **Figure S5** gives an example of the synchronization process. It is clear that before deformation, f_H is -0.016 and -0.006 for lamellae and (040) reflection. The small negative deviation is due to the slight compression force caused by the thermal expansion of the sample under 75 ^{o}C. Upon stretching, both f_H values increase linearly in the elastic deformation region. Via this process, the onset of the mechanical

test and the onset of SAXS/WAXS measurements could be well synchronized. In **Figure S5**, one can also see that at the same displacement, the growth of f_H from the lamellae side is 4 times larger than that from the (040) reflections. This is because the constraint force from the lattice is much higher compared to the rigidity of the amorphous phase, which benefits a larger rotation angle of the lamella.

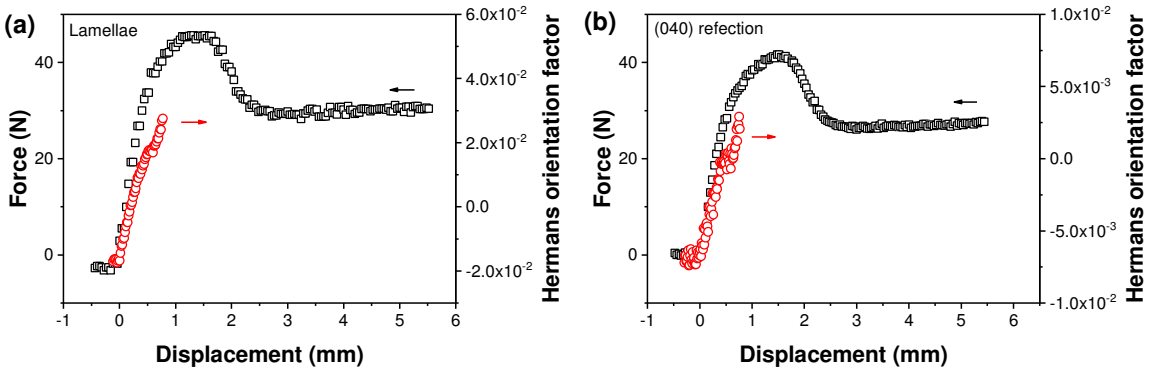

Figure S5 (a) Engineering force-displacement curve (square) and lamellae Hermann's orientation factor (circle) of PPna uniaxial stretching at 75 ^{o}C; **(b)** Engineering force-displacement curve (square) and (040) reflection Hermann's orientation factor (circle) of PPna uniaxial stretching at 75 ^{o}C.

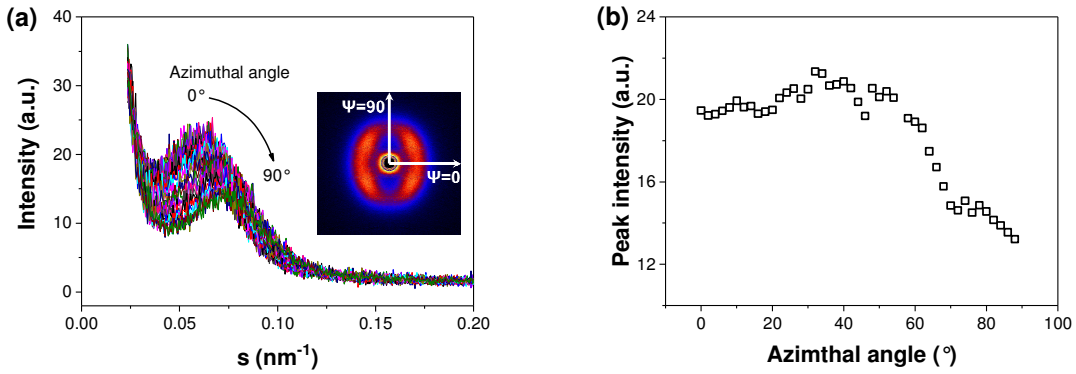

Figure S6 (a) The 1D-SAXS curve at different azimuthal angle with an interval of 2° from the "four-arc" scattering pattern; **(b)** The intensity at the peak position as a function of azimuthal angle.

In **Figure S7** the dependence of the reciprocal of the lamellae thickness ($1/L_c$) on the stretching temperature is plotted. The lamellae thickness increases as the stretching temperature is increased. Recently, the stretching induced crystallization was investigated by Men.[3] In his work, the stretching induced crystallization was proposed to be mediated by a mesomorphic phase, which was based on the crystallization proposed by Strobl.[4] For the crystallization via a mesomorphic phase, the crystallization line could be defined as[4]

(3) $$T_{mc}^{\infty} - T \approx \frac{2(\sigma_{ac_n} - \sigma_{am})}{\Delta H_{cm}} \frac{\Delta z}{L_c}$$

where ΔH_{cm} is the heat of transition from mesomorphic phase to crystalline phase, Δz is the stem length increment per structural unit, and σ_{ac_n} and σ_{cm} denote the surface free energy of the native crystal layer and the mesomorphic layer, respectively. The slope in this study is larger than the one obtained by Men.[3] The difference may be caused by the higher molecular weight iPP used in this study, which increases the surface-free energy of the native crystal formed from the mesomorphic phase.[5]

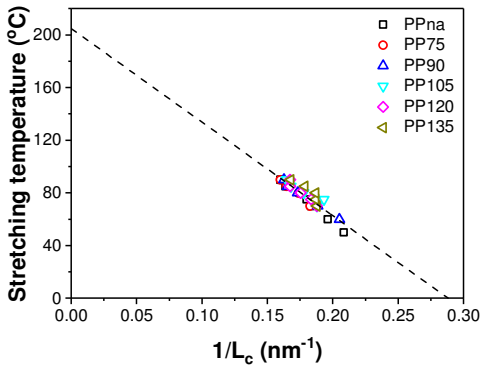

Figure S7 Dependence of the reciprocal of the lamellae thickness ($1/L_c$) on the stretching temperatures.

The evolution of the peak position and peak width of (040) crystal plane during stretching are provided in **Figure S8a** and **b** In the strain range of 0~0.1, an instance increase of the peak position and peak width can be found. Since the peak position and peak width are obtained by the vertical cut from the 2D-WAXS patterns, the increase of the peak position of (040) crystal plane indicates that the lamellae with their ***c***-axis aligned along the loading direction are subjected to a compression force in the ***b***-axis direction. In the same range the peak position changes less than 1 % (see **Figure S8a**), suggesting a very small deformation of the crystallites. Consequently, the crystallite size is mainly reflected by the width of the peaks. In the strain range of 0.1~0.95, the peak width increases continually with strain (see **Figure S8b**), which is the result of lamellar tilting and intra-lamellar slip. By lamellar tilting and intra-lamellar slip, the initial lamellae are fragmented into lamellae blocks.

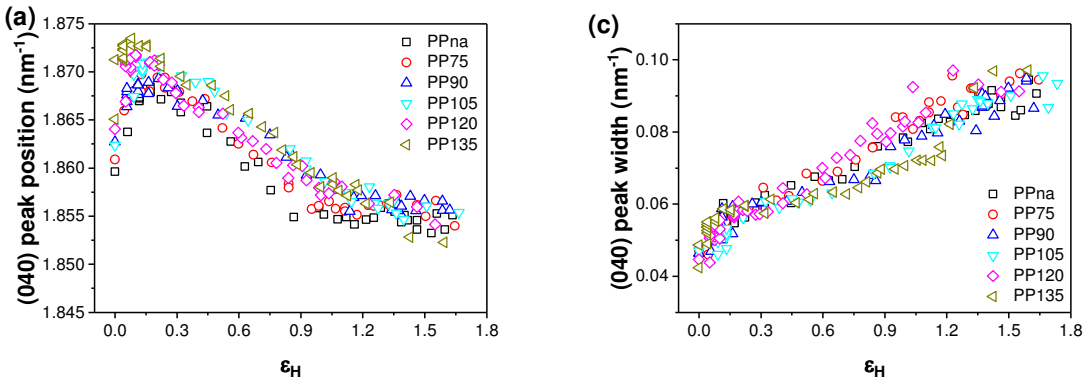

Figure S8 (a) Plots of the peak position of (040) crystal plane and **(b)** plots of the peak width of (040) crystal plane as a function of ε_H during stretching.

The molecular origin of the void formation was studied by different groups recently. In the work by Men,[6] the void formation at large strain deformation was proposed to be a consequence of the disentanglement of the highly oriented amorphous network initiated by the breaking of

interfibrillar tie chains. Whereas, Ge[7] proposed that disentanglement is not geometrically necessary to accommodate void propagation because the chains in deformed glassy polymers are constrained by their rheological tubes rather than by entanglements that act like discrete cross-links. And Ge proposed that clustering of the polymer chains into fibrils may be the mechanism of void formation without entanglement loss.[7]

To know whether polymer chains were broken or not after uniaxial stretching, the molecular weight of the un-stretched iPP and stretched iPP with voids inside was determined by DAWN Heleos-II (Wyatt technology). The solvent used was 1,2,4-trichlorobenzene (stabilized with 0.1% BHT) and the flow rate was 1.0 ml min^{-1}. The molecular weight of PP135 with and without abundant cavitation is given in **Figure S9**. It can be found that the molecular weight of the two samples overlaps with each other, suggesting that the breaking of polymer chains is not the compulsive condition for void formation. However, the conclusion by Ge was deduced from crazing behavior of the glassy polymer. In this study, the sample was stretched at 75 ^{o}C which is much higher than the glass transition (around 0 ^{o}C for crystallized iPP). At this temperature, the chains in the amorphous phase of the polymer will have a higher mobility. Therefore, no stringent conclusion concerning whether the polymer chains are disentangled or not can be inferred from **Figure S9**. More work dealing with the molecular origin of void formation in semicrystalline polymers should be performed in the future.

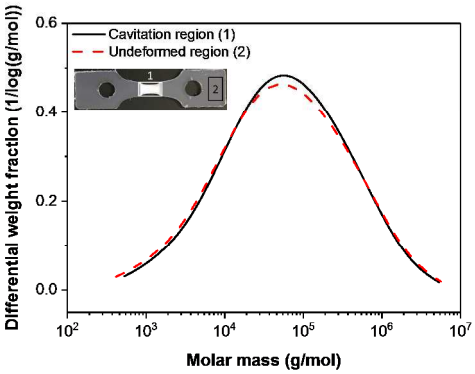

Figure S9 The molecular weight of iPP from the un-deformed region and the cavitation region.

Reference

1. Millot, C.; Séguéla, R.; Lame, O.; Fillot, L. A.; Rochas, C.; Sotta, P. Tensile Deformation of Bulk Polyamide 6 in the Preyield Strain Range. Micro–Macro Strain Relationships via in Situ SAXS and WAXS. *Macromolecules* **2017,** *50*, 1541-1553.

2. Desper, C. R.; Stein, R. S. Measurement of Pole Figures and Orientation Functions for Polyethylene Films Prepared by Unidirectional and Oriented Crystallization. *J. Appl. Phys.* **1966,** *37*, 3990-4002.

3. Lu, Y.; Wang, Y.; Chen, R.; Men, Y. Crystallization and melting of isotactic polypropylene crystallized from quiescent melt and stress-induced localized melt. *J. Polym. Sci. B: Polym. Phys.* **2017,** *55*, 957-963.

4. Strobl, G. Colloquium: Laws controlling crystallization and melting in bulk polymers. *Rev. Mod. Phys.* **2009,** *81*, 1287-1300.

5. Wang, Y.; Lu, Y.; Jiang, Z.; Men, Y. Molecular Weight Dependency of Crystallization Line, Recrystallization Line, and Melting Line of Polybutene-1. *Macromolecules* **2014,** *47*, 6401-6407.

6. Lu, Y.; Wang, Y.; Chen, R.; Zhao, J.; Jiang, Z.; Men, Y. Cavitation in Isotactic Polypropylene at Large Strains during Tensile Deformation at Elevated Temperatures. *Macromolecules* **2015,** *48*, 5799-5806.

7. Ge, T.; Tzoumanekas, C.; Anogiannakis, S. D.; Hoy, R. S.; Robbins, M. O. Entanglements in Glassy Polymer Crazing: Cross-Links or Tubes? *Macromolecules* **2017,** *50*, 459-471.